Published in final edited form as:
Hum Mutat. 2012 June ; 33(6): 989–997. doi:10.1002/humu.22058.

Novel Mutations in the *KCND3*-Encoded Kv4.3 K+ Channel Associated with Autopsy-Negative Sudden Unexplained Death

John R. Giudicessi[1,2,3,4,†], **Dan Ye**[1,2,3,†], **Chad J. Kritzberger**[4], **Vladislav V. Nesterenko**[5], **David J. Tester**[1,2,3], **Charles Antzelevitch**[5], and **Michael J. Ackerman**[1,2,3,*]

[1]Division of Cardiovascular Diseases, Department of Medicine, Windland Smith Rice Sudden Death Genomics Laboratory, Mayo Clinic, Rochester, Minnesota

[2]Division of Pediatric Cardiology, Department of Pediatrics, Windland Smith Rice Sudden Death Genomics Laboratory, Mayo Clinic, Rochester, Minnesota

[3]Department of Molecular Pharmacology and Experimental Therapeutics, Windland Smith Rice Sudden Death Genomics Laboratory, Mayo Clinic, Rochester, Minnesota

[4]Mayo Medical School, Mayo Clinic, Rochester, Minnesota

[5]Masonic Medical Research Laboratory, Utica, New York

Abstract

Heritable arrhythmia syndromes, including Brugada syndrome (BrS) and idiopathic ventricular fibrillation (IVF), may serve as the pathogenic basis for autopsy-negative sudden unexplained death (SUD) and sudden infant death syndrome (SIDS). Emerging evidence has linked perturbations in the transient outward current (I_{to}) conducted by the *KCND3*-encoded Kv4.3 pore-forming α-subunit to BrS or IVF. However, the contribution of *KCND3* mutations to autopsy-negative SUD/SIDS is unknown. To investigate the potential association between *KCND3* and SUD/SIDS, mutational analysis of *KCND3* was conducted in 123 SUDS and 292 SIDS victims using polymerase chain reaction, denaturing high-performance liquid chromatography, and direct sequencing. Overall, one SIDS case (<1.0%) and two SUDS cases (1.6%) harbored potentially pathogenic mutations in *KCND3*. The novel p.Val392Ile, p.Ser530Pro, and p.Gly600Arg mutations involved highly conserved residues and were absent in 1,560 reference alleles. Although the SIDS-associated p.Ser530Pro mutation demonstrated a wild-type (WT) electrophysiological phenotype when heterologously expressed, the SUDS-associated p.Val392Ile and p.Gly600Arg mutations significantly increased peak current density at +40 mV in comparison with WT by 100.4% ($P < 0.05$) and 50.4% ($P < 0.05$), respectively. p.Val392Ile also slowed recovery from inactivation 3.6-fold, indicating a mixed electrophysiological phenotype. This is the first report indicating that *KCND3* may serve as a rare genetic substrate in the pathogenesis of SUDS but not SIDS cases.

Keywords

KCND3; arrhythmia; sudden death; ion channels; pediatrics

[*]Correspondence to: Michael J. Ackerman, Division of Cardiovascular Diseases, Department of Medicine, Windland Smith Rice Sudden Death Genomics Laboratory, Mayo Clinic, Guggenheim 501, Rochester, MN 55905. ackerman.michael@mayo.edu.
[†]These authors contributed equally to the research and are joint first authors.

Disclosure Statement: M.J.A. is a consultant for Transgenomic. Intellectual property derived from M.J.A.'s research program resulted in license agreements in 2004 between Mayo Clinic Health Solutions (formerly Mayo Medical Ventures) and PGxHealth (formerly Genaissance Pharmaceuticals and now recently acquired by Transgenomic).

Introduction

Within the United States alone, an estimated 300,000 people succumb to sudden cardiac arrest annually [Chugh et al., 2008; Zheng et al., 2001]. Although the preponderance of sudden cardiac death (SCD) occurs in the elderly often secondary to atherosclerotic coronary artery disease, each year several thousand individuals under the age of 40 years, including infants, die without warning, facilitating the need for a detailed medicolegal examination [Liberthson, 1996]. In approximately two-thirds of these young sudden death victims, an identifiable, often heritable, cardiac abnormality such as hypertrophic cardiomyopathy, ruptured aortic aneurysm, or acute myocarditis is identified during the postmortem examination [van der Werf et al., 2010]. However, in up to one-third of cases involving previously healthy individuals between the ages of 1 and 40 years with structurally normal hearts, the cause of death remains unexplained following autopsy and represents a clinical entity referred to as autopsy-negative sudden unexplained death syndrome (SUDS) [van der Werf et al., 2010]. Additionally, an estimated 60–80% of sudden deaths involving infants under the age of 1 year remain unexplained following autopsy and are labeled as autopsy-negative sudden infant death syndrome (SIDS) cases [Arnestad et al., 2002; Cote et al., 1999]. Although the pathogenic mechanisms underlying autopsy-negative SIDS and SUDS remain largely unexplained, it is estimated that 10–20% of SIDS and 30% of SUDS stem from potentially lethal cardiac channelopathies such as long QT syndrome (LQTS), catecholaminergic polymorphic ventricular tachycardia (CPVT), and Brugada syndrome (BrS) that are undetectable by a standard medicolegal autopsy [Klaver et al., 2011; Tester and Ackerman, 2005, 2007].

The transient outward current (I_{to}) that mediates early (phase 1) repolarization and is conducted by the Kv4.3 pore-forming α-subunit encoded by *KCND3* (MIM# 605411) in humans remains central to the "the repolarization disorder" theory of the electrocardiographic and arrythmogenic manifestations of BrS. Insufficient sodium (I_{Na})- or calcium (I_{Ca})-inward depolarizing current or the presence of a genetically enhanced potassium (I_{to} or I_{K-ATP})-outward repolarizing current coupled with an intrinsic right ventricular (RV) I_{to}-mediated transmural voltage gradient (epicardium > endocardium) is hypothesized to result in a net outward shift in current, heterogeneous loss of the action potential dome, ST segment elevation on electrocardiogram (ECG), and the development of potentially fatal polymorphic ventricular tachycardia or ventricular fibrillation via phase II reentry [Antzelevitch and Yan, 2010]. The recent identification of BrS-associated I_{to} gain-of-function mutations in *KCND3*-encoded Kv4.3 [Giudicessi et al., 2011] and a BrS-associated loss-of-function mutation in the Kv4.3-negative regulator *KCNE3*-encoded MiRP2 that significantly increases I_{to} current [Delpon et al., 2008] have served to strengthen the role of the I_{to} current in sudden death-predisposing J wave syndromes.

Given the emerging role of the I_{to} current in the pathogenesis of sudden death-predisposing disorders such as BrS and idiopathic ventricular fibrillation (IVF), we hypothesized that mutations in *KCND3* may confer risk for lethal ventricular arrhythmias and as such may serve as the underlying pathogenic substrate for some cases of autopsy-negative SUDS and SIDS. Thus, we sought to determine the spectrum and prevalence of *KCND3* mutations within a cohort of 123 unrelated SUDS victims and a cohort of 296 unrelated SIDS victims.

Materials and Methods

Medical Examiner/Coroner Referred Cohort of SUDS

One hundred and twenty three cases of SUDS (Table 1) were referred for molecular autopsy. This SUDS cohort also included 21 cases of unexplained drowning. In order to be accepted

as a SUDS case, by definition, the death had to occur after the first year of life and be sudden, unexpected, and unexplained following the conclusion of a detailed medicolegal examination. Although no upper age limit was specified to accept a sample for postmortem genetic testing, 112 of the 123 cases were between 1 and 40 years of age. Seven decedents were in their 40s, three were in their 50s, and a single SUD victim was in his 60s. Those decedents with a documented premortem diagnosis of a cardiac channelopathy in either himself or herself or in a blood relative were excluded from this study. These SUDS samples had been analyzed previously for all major channelopathic genes (*KCNQ1*, *KCNH2*, *SCN5A*, *CACNA1C*, *CACNB2*, *SCN5A*, and *RYR2*) and a number of minor channelopathic genes (*KCNE1*, *KCNE2*, *KCNE3*, *KCNJ2*, *KCNJ8*, *CAV3*, *GPD1L*, *SCN1B*, *SCN3B*, *SCN4B*, *GJA1*, and *ANK2*). The Mayo Foundation Institutional Review Board approved the present study. Although informed consent is waived for studies involving decedents, written informed consent was obtained from the decedent's parents or appropriate next of kin.

Population-Based Cohort of SIDS

Two hundred and ninety two cases derived from several population-based cohorts of unexplained infant deaths (Table 2) were referred for molecular autopsy. SIDS was defined as an autopsy-negative SUD occurring during the first year of life. Infants whose deaths clearly resulted from asphyxia or a specific disease process were excluded. The Mayo Foundation Institutional Review Board approved the present study as an anonymous necropsy study. As a result, only limited medical information pertaining to sex, ethnicity, and age at time of death was available.

Control Populations

DNA from a cohort of 780 (680 Caucasian and 100 African American) ostensibly healthy individuals was obtained from the Coriel Cell Repository and European Collection of Cell Cultures. These samples were used to assess allelic frequency for all identified nonsynonymous variants.

Postmortem Genetic Analysis of *KCND3*

Genomic DNA was extracted from autopsy blood using Purgene DNA extraction kits (Gentra Systems Inc., Minneapolis, MN, USA) or from frozen necropsy tissue using the Qiagen DNeasy Tissue Kit (Qiagen, Inc., Valencia, CA, USA). Comprehensive mutational analysis of the entire coding region (seven translated exons) and splice junctions of the *KCND3* long isoform was accomplished in cases and controls using polymerase chain reaction (PCR), denaturing high-performance liquid chromatography (DHLPC), and direct DNA sequencing as previously described [Giudicessi et al., 2011]. Nucleotide numbering reflects cDNA numbering with +1 corresponding to the A of the translation initiation codon of *KCND3* (Ref Seq. NM_004980.4) encoding the Kv4.3 long isoform. Amino acids were numbered relative to the protein reference sequence NP_004971.2. Primer sequences, PCR conditions, and DHPLC conditions are available upon request. The variants have been submitted to the Leiden database for *KCND3* (http://www.LOVD.nl/KCND3).

In order to be considered a putative SIDS- or SUDS-associated mutation, the genetic variant of interest had to: (1) be a nonsynonymous variant (all synonymous nucleotide substitutions were excluded for the purposes of this study), (2) involve a residue highly conserved across species, (3) be absent from 1,560 healthy reference alleles derived from 680 Caucasian and 100 African American controls, and (4) display a functionally perturbed, potentially proarrhythmic cellular electrophysiological phenotype.

KCND3 and *KCNIP2* Mammalian Expression Vectors and Mutagenesis

Wild-type (WT) human *KCND3* (Kv4.3 α-subunit, NM_004980.4) and *KCNIP2* (KChIP2 β-subunit, NM_173193.2) cDNA were subcloned into pIRES2–EGFP (Clontech, Mountain View, CA, USA) and pIRES2–dsRed2 (Clontech) to produce the pIRES2–*KCND3*^{WT}–EGFP and pIRES2–*KCNIP2*^{WT}–dsRed2 mammalian expression vectors as previously described [Giudicessi et al., 2011]. The identified mutations were engineered into pIRES2–*KCND3*^{WT}–EGFP using the Quikchange XL Site-Directed Mutagenesis Kit (Stratagene, La Jolla, CA, USA). The integrity of all mammalian expression vectors was confirmed using direct DNA sequencing.

HEK293 Cell Culture and Transfection

HEK293 cells were cultured in minimum essential medium supplemented with 1% nonessential amino acid solution, 10% horse serum, 1% sodium pyruvate solution, and 1.4% penicillin/streptomycin solution. All cells were plated in T25 flasks and stored in a 5% CO_2 incubator at 37°C for 24 hr. Heterologous expression of Kv4.3 and KChIP2 was accomplished by cotransfecting 0.5 μg of pIRES2–*KCND3*^{WT}–EGFP, or pIRES2–*KCND3*^{Mut}–EGFP with 1.5 μg pIRES2–*KCNIP2*^{WT}–dsRed2 using 5 μl of Lipofectamine transfection reagent (Invitrogen, Carlsbad, CA, USA) in Gibco® OPTI-MEM media (Invitrogen). Cells exhibiting both green fluorescence and red fluorescence at 24 hr posttransfection were selected for electrophysiological experiments.

Electrophysiological Measurements and Data Analysis

Standard whole cell patch clamp technique was used to measure WT, p.Val392Ile, p.Ser530Pro, or p.Gly600Arg Kv4.3 plus KChIP2 currents at room temperature (22–24°C) with the use of an Axopatch 200B amplifier, Digidata 1440A, and pClamp version 10.2 software (Axon Instruments, Foster City, CA, USA). The extracellular (bath) solution contained (mmol/L) 140 NaCl, 4 KCl, 2 $CaCl_2$, 1 $MgCl_2$, and 10 HEPES, pH adjusted to 7.4 with NaOH. The pipette solution contained (mmol/L) 110 KCl, 31 KOH, 10 EDTA, 5.17 $CaCl_2$, 1.42 $MgCl_2$, 4 MgATP, and 10 HEPES, pH adjusted to 7.2 with KOH following established protocols [Giudicessi et al., 2011]. Microelectrodes were pulled on a P-97 puller (Sutter Instruments, Novato, CA, USA) and fire polished to a final resistance of 2–3 MΩ. Series resistance was compensated by 80–85%. Currents were filtered at 5 kHz and digitized at 10 kHz. The voltage dependence of activation, inactivation, and recovery from inactivation were determined using voltage-clamp protocols described in the figure legend. Data were analyzed using Clampfit (Axon Instruments), Excel (Microsoft, Redmond, WA, USA), and fitted with Origin 8 (OriginLab Corporation, Northampton, MA, USA).

Voltage-dependent inactivation curve was fitted with a Boltzmann function: $I/I_{,max} = \{1+\exp[(V - V_{1/2})/k]\}^{-1}$, where $V_{1/2}$ and k are the half-maximal voltage of inactivation and the slope factor, respectively. Recovery from inactivation was fitted with a one-exponential function: $y = y_0+[A_1 \exp(-x/\tau_1)]$ where A_1 indicates the fractions of recovery from inactivation, τ_1 indicates the time constant for recovery from inactivation. Inactivation time constants for each voltage step were determined by fitting a monoexponential function to current decay. Total charge as a function of voltage was obtained by measuring the area under curve during the first 500 ms of each voltage step.

Simulated Ventricular Epicardial Action Potentials

Both RV and left ventricular (LV) epicardial action potentials were simulated using a Luo–Rudy II (LRII) AP model, modified to include the I_{to} current as previously described [Dumaine et al., 1999; Gima and Rudy, 2002; Giudicessi et al., 2011]. The maximal conductance of the calcium current (I_{CaL}) was decreased by 30% to compensate for the

larger driving force during the AP notch. The RV I_{to} maximal conductance was set to 1.3 mS/μF for WT, 2.47 mS/μF for p.Val392Ile, and 1.92 mS/μF for p.Gly600Arg, whereas LV I_{to} maximal conductance was set to 0.5 mS/μF for wild-type, 0.95 mS/μF for p.Val392Ile, and 0.74 mS/μF for p.Gly600Arg to reflect the reduced expression of *KCND3* in the LV epicardium.

The LRII model simulates cardiac APs at 37°C, leading to much faster kinetics compared with room temperature. Therefore, much smaller values for inactivation time constants were used for simulations: 10.1 ms for wild-type, 24.0 ms for p.Val392Ile, and 12.4 ms for p.Gly600Arg, that is, the time constants of inactivation were increased by 138% for the p.Val392Ile mutant and 23% for the p.Gly600Arg mutant. All modeled parameters were in agreement with experimentally derived values. Epicardial APs were simulated assuming equal heterozygous expression of WT and mutant (either p.Val392Ile or p.Gly600Arg)-containing alleles. Therefore, the simulated I_{to} current consisted of an equal (50–50%) mixture of the WT and corresponding mutant current. As p.Ser530Pro exhibited WT characteristics, no simulated action potentials were obtained for this rare amino acid substitution.

Statistical Analysis

All data points represent the mean value and bars represent the standard error of the mean. Determination of statistical significance between two groups was accomplished using a Student's *t*-test. One-way analysis of variance was used among multiple group comparison. A P value of <0.05 was considered statistically significant.

The authors had full access to take full responsibility for the integrity of the data. All authors have read and agreed to the manuscript as written.

Results

Postmortem Mutational Analysis

Overall, the molecular interrogation of *KCND3* revealed three distinct, rare missense mutations in 1/292 SIDS cases (<1.0%) and 2/123 SUDS cases (1.6%) (Table 3 and Fig. 1A and B). None of the mutations was detected in 1,560 in-house reference alleles, p.Val392Ile and p.Ser530Pro were both absent in the dbSNP134 and 1,000 genomes public variant databases, whereas p.Gly600Arg (rs149344567:T/C) was detected in a single individual of European descent in dbSNP134 but was absent from 1,000 genomes. All mutations involved residues highly conserved in placental mammals, including dog, mouse, rat, cow, and horse, that localize to the sixth transmembrane (p.Val392Ile) or carboxyl (C)-terminus (p.Ser530Pro and p.Gly600Arg) of the Kv4.3 channel (Fig. 1C and D). The p.Gly600Arg mutation was discovered previously in a living subject with clinically diagnosed BrS [Giudicessi et al., 2011].

SUDS and SIDS Cases Harboring *KCND3* Amino Acid Altering Genetic Variation

The p.Val392Ile-positive SUDS case, a 20-year-old male with a history of syncopal episodes, was brought to the emergency room in full cardiopulmonary arrest after being discovered unresponsive in bed by his parents. The decedent did not show any signs of overt illness in the days leading up to his death. The parents immediately initiated cardiopulmonary resuscitation (CPR) and an emergency response team was dispatched to the home. There was no report of cardiac activity or rhythm during transport and upon arrival in the Emergency Department, there was no palpable pulse. The decedent underwent five rounds of synchronized cardioversion to no avail and was declared dead shortly thereafter. A urine drug and toxin screen was negative. No premortem ECGs were available

and the decedent's past medical history was largely unremarkable aside from two suspicious syncopal episodes as a teenager. There was no documented history of SUD or arrhythmia-related cardiac events in the family and screening 12-lead ECGs of the parents and sister of the decedent were all reportedly normal. Although family members agreed to undergo a cardiovascular examination, they declined to submit samples for genetic testing and thus the familial or sporadic status of the p.Val392Ile mutation could not be established.

The p.Gly600Arg-positive SUD index case, a 23-year-old accomplished male athlete with no significant medical history, was brought to the emergency room in full cardiopulmonary arrest after being discovered at the bottom of a swimming pool while swimming laps at a university recreation center. Pool staff initiated CPR and an automatic external defibrillator was deployed before emergency response crews arrived. The patient was resuscitated prior to arrival in the emergency room and was transferred to the ICU where he was declared brain dead the next morning. No premortem ECGs were available and the decedent had no documented history of palpitations or syncope. Surviving family members declined participation in this study and thus a family history of SCD is unknown.

Because of the blinded and anonymous nature of the population-based SIDS cohort, it was not possible to obtain further information on the p.Ser530Pro-positive SIDS case besides the basic demographic information listed in Table 3.

Functional Characterization of SIDS- and SUDS-Associated Mutations in Kv4.3

Figure 2A displays the representative tracings of WT, p.Val392Ile, p.Ser530Pro, or p.Gly600Arg Kv4.3 heterologously coexpressed with WT KChIP2 in HEK293 cells. Analysis of the current-voltage relationship indicated that p.Val392Ile plus KChIP2 dramatically increased I_{to} current density from −20 mV to +40 mV ($n = 16$, $P < 0.05$) and p.Gly600Arg plus KChIP2 significantly increased I_{to} current density from +10 mV to +40 mV ($n = 11$, $P < 0.05$) compared with WT Kv4.3 plus KChIP2 ($n = 16$, Fig. 2B). Furthermore, p.Val392Ile significantly increased peak current density at +40 mV by 100.4% from 193.8 ± 24.1 (WT, $n = 16$) to 388.3 ± 46.8 (p.Val392Ile, $n = 16$, $P < 0.05$) and p.Gly600Arg significantly increased peak current density at +40 mV by 50.3% to 291.3 ± 40.0 (p.Gly600Arg, $n = 11$, $P < 0.05$, Fig. 2C), indicating a marked gain-of-function electrophysiological phenotype for the p.Val392Ile and p.Gly600Arg mutant Kv4.3 currents. However, in comparison with WT, the current density for p.Ser530Pro plus KChIP2 remained unchanged.

The p.Val392Ile mutation plus KChIP2-WT also exhibited significantly slower inactivation tau across the 0–40 mV range compared with WT Kv4.3 plus KChIP2 by 138.0% from 78.6 ± 1.9 ms (WT at 40 mV, $n = 16$) to 187.1 ± 11.4 ms (p.Val392Ile at 40 mV, $n = 16$, $P < 0.05$, Fig. 3A). Consequently, the I_{to} total charge associated with p.Val392Ile plus KChIP2 markedly increased by 298.7% at 40 mV ($n = 16$, $P < 0.05$) compared with WT Kv4.3 plus KChIP2 ($n = 16$, Fig. 3B).

Steady-state inactivation was assessed by a standard two-pulse voltage-clamp protocol (see inset Fig. 3C and figure legend) and steady-state inactivation curves were fit using a Boltzmann function. Although p.Ser530Pro did not significantly alter the inactivation kinetics of I_{to} compared with WT, p.Val392Ile shifted $V_{1/2}$ of inactivation by −3.0 mV from −22.9 ± 0.6 mV (WT, $n = 11$) to −25.9 ± 0.5 mV(p.Val392Ile, $n = 12$, $P < 0.05$, Fig. 3C). The respective k (slope factor) remained unchanged for all mutations. The time constants for the recovery from inactivation assessed using a two-pulse protocol (see inset Fig. 3D and figure legend) were 55.1 ± 1.6 ms for Kv4.3-WT plus KChIP2 ($n = 5$). However, p.Val392Ile plus KChIP2 slowed recovery from inactivation by 360.9% to 254.0 ± 21.6 ms

(p.Val392Ile, $n = 6$, $P < 0.05$). Akin to their WT-like peak current and inactivation kinetics, p.Ser530Pro was WT with respect to recovery from inactivation as well.

Simulated Effect of p.Val392Ile and p.Gly600arg on the RV and LV Epicardial Action Potential

Simulated I_{to} current traces under standard voltage-clamp conditions indicate that the homozygous expression of p.Val392Ile or p.Gly600Arg increases peak current density by 100.4% and 50.1%, respectively, and that p.Val392Ile and p.Gly600Arg slows the inactivation time constant by 138% and 23.0%, respectively, relative to WT Kv4.3 (Fig. 4A). The total charge carried by the simulated I_{to} was increased 355% by p.Val392Ile relative to WT and 84% by p.Gly600Arg relative WT. The computer simulations recapitulated the peak current density, inactivation tau, and total charge expected to be associated with the experimentally derived p.Val392Ile and p.Gly600Arg currents across the 0 to +40 mV range.

Simulated RV epicardial action potentials using p.Val392Ile, p.Gly600Arg, and WT I_{to} currents were used to assess the ability of the p.Val392Ile and p.Gly600Arg mutants to precipitate the loss of the AP dome in a modified LRII AP model. As described in the *Materials and Methods* section, the model assumes heterozygous expression of the mutant channels, so that 50% of the total I_{to} is due to WT current and another 50% comes from either p.Val392Ile or p.Gly600Arg mutant current. After several cycles of simulation at a basic cycle length of 800 ms to allow for the proper reequilibration of intracellular Ca^{2+} concentrations, the simulated action potentials containing both p.Val392Ile and p.Gly600Arg mutant I_{to} currents displayed a marked and stable loss of the AP dome (Fig. 4B).

In contrast to the RV epicardium, the dramatic increase in I_{to} total charge conducted by p.Val392Ile failed to cause the loss of the AP dome when superimposed on the lower baseline I_{to} maximal conductance associated with the LV epicardium. However, the increased I_{to} maximal conductance associated with p.Val392Ile interferes with the inactivating calcium current during the second upstroke resulting in the delayed development of the AP dome, prolongation of the LV epicardial AP, and creation of a strong heterogeneous distribution of repolarization (Fig. 5).

Discussion

Emerging Role of I_{to} Perturbations in SCD

Previous studies estimate that nearly one-third of autopsy-negative SUD cases referred for postmortem genetic testing harbor putative pathogenic mutations in cardiac channelopathy-susceptibility genes [Tester and Ackerman, 2007; Tester et al., 2004]. Furthermore, a thorough cardiologic examination and targeted genetic analysis of surviving relatives identified an underlying heritable cardiac channelopathy (LQTS, CPVT, or BrS) in nearly 40% of families with a history of autopsy-negative SUDS [Tan et al., 2005]. Thus, the identification of a heritable cardiac channelopathy in the deceased provides an important opportunity to identify those surviving relatives at risk and take appropriate measures to prevent additional tragic sudden deaths. In this present study, we provide the molecular and functional evidence necessary to add I_{to} gain-of-function mutations in the *KCND3*-encoded Kv4.3 potassium channel as a novel pathogenic substrate for autopsy-negative SUD.

Although the presence of a strong unopposed I_{to} current in the RV epicardium occurring as sequelae of loss-of-function mutations within Nav1.5 and Cav1.2 macromolecular complex components has long been hypothesized to contribute to electrocardiographic and arrhythmogenic manifestation of J wave syndromes, the molecular and functional evidence

to demonstrate a direct role of genetically enhanced I_{to} current in the pathogenesis of these diseases has been slow to emerge. The identification of a rare BrS-associated loss-of-function mutation in the Kv4.3 negative modulating β-subunit *KCNE3*-encoded MiRP2 [Delpon et al., 2008] and an IVF-associated promoter variant linked to the increased expression of the Kv4.3 β-subunit *DPP6*-encoded DPP6 [Alders et al., 2009] provided the initial evidence that a genetic enhancement of the I_{to} current may contribute to the pathogenesis of sudden death-predisposing cardiac arrhythmia syndromes. Most recently, our group identified two novel gain-of-function mutations in the Kv4.3 pore-forming α-subunit in 2/86 genetically elusive BrS cases that were predicted to cause the stable loss of the AP dome, providing the first direct evidence that I_{to} gain-of-function mutations in the Kv4.3 α-subunit could potentially contribute to the phenotypic expression of BrS [Giudicessi et al., 2011]. Interestingly, while *KCNE3* loss-of-function, *DPP6* overexpression, and *KCND3* gain-of-function mutations are all postulated to enhance the I_{to} current, only patients with *KCNE3* and *KCND3* mutations presented with a discernable phenotype (BrS) on ECG. Although the uniform expression of *DPP6* in epicardium and endocardium of the heart [Alders et al., 2009] and the modest increase in the I_{to} shown to accompany additional free DPP6 β-subunits [Soh and Goldstein, 2008] may not necessarily alter the I_{to} transmural gradient enough to produce a distinct ECG phenotype, the malignant IVF phenotype associated with the Dutch *DPP6* founder mutation indicates that perturbation of I_{to} may contribute to arrhythmogenesis and SUD via yet to be discovered cellular mechanisms.

Although three rare missense mutations (p.Val392Ile, p.Ser530Pro, and p.Gly600Arg) were identified in one SIDS and two SUDS subjects, the combined molecular and functional evidence justify a classification for only p.Val392Ile and p.Gly600Arg as SUD-predisposing pathogenic mutations. Although rare and conserved across species, p.Ser530Pro is concluded to be a functionally WT-like variant without definite pathogenic influence. Of course, we cannot rule out the possibility that this variant perturbs the larger Kv4.3 macromolecular complex that conducts the I_{to} current in vivo. Nevertheless, no definite pathogenic *KCND3* mutations in SIDS cases have been found thus far.

Molecular Mechanisms Underlying SUDS-Associated *KCND3* Mutations

The p.Val392Ile Kv4.3 channel dramatically increases both peak I_{to} current density (100.4%) and total charge (298.7%), while slowing decay time (138.0%), indicating a BrS-like I_{to} gain-of-function. Interestingly, pVal392Ile also slows the recovery from inactivation by 360.9%. However, even the slowly recovering I_{to} current conducted by p.Val392Ile Kv4.3 is expected to recover completely at physiologically normal heart rates. Although p.Val392Ile clearly has a mixed electrophysiological phenotype, it seems unlikely that p.Val392Ile manifests itself as an I_{to} “loss-of-function” in patients under normal physiologic circumstances. Computer simulations employing a modified LRII AP model that incorporates a 50–50% mixture of WT and p.Val392Ile currents demonstrated that the increase in I_{to} current density (100.4%) together with the significant slowing of I_{to} decay time (138.0%) associated with the heterozygous expression of p.Val392Ile in the heart is capable of producing a BrS-like stable loss of the AP dome in the RV epicardium. Interestingly, simulations employing a smaller I_{to} maximal conductance intended to model the LV epicardial action potential did not demonstrate loss of the AP dome, but rather displayed a significant prolongation of the LV epicardial action potential duration (APD).

Thus, p.Val392Ile is the first Kv4.3 mutation reported with functional derangements, suggesting a mixed electrophysiological phenotype and therefore the potential for a mixed or overlapping arrhythmia phenotype. The p.Val392Ile-positive SUDS case’s death during sleep is consistent with a BrS-like I_{to} gain-of-function as the primary underlying etiology and a BrS-triggered fatal arrhythmia as the decedent’s chief arrhythmia phenotype.

Unfortunately, due to a lack of medical history including premortem ECGs on the p.Val392Ile-positive SUDS index case, we are unable to characterize the decedent's arrhythmia phenotype unambiguously. It is conceivable that the potential contributions of I_{to} gain-of-function-mediated prolongation of LV APD and/or the significantly delayed I_{to} recovery from inactivation associated with p.Val392Ile could have contributed to a unique arrhythmia profile.

As previously reported, p.Gly600Arg significantly increased both peak current density and total charge across the 0 to +40 mV range and slowed I_{to} inactivation by 23%, indicating an I_{to} gain-of-function consistent with the phenotypic expression of BrS [Giudicessi et al., 2011]. Interestingly, unlike the previously reported p.Gly600Arg-positive BrS index case that was discovered unresponsive in bed, this p.Gly600Arg-positive SUDS victim suffered an apparent cardiac event while swimming laps at a university recreation center. Although an increase in vagal tone and the resulting autonomic imbalance that occurs during sleep and rest is widely believed to play a pathophysiologic role in the development of ventricular arrhythmias in BrS patients, recent studies have demonstrated that exercise aggravates underlying ECG abnormalities such as ST segment elevation and heart-rate-corrected QT interval that are often associated with an increase risk of adverse cardiac events in BrS [Amin et al., 2009; Makimoto et al., 2010]. Furthermore, the opening of predominantly epicardial expressed K_{ATP} channels in the heart as a result of the physiologic metabolic stress encountered during endurance swimming [Zingman et al., 2007] could exacerbate the underlining genetically enhanced I_{to}-mediated transmural voltage gradient, precipitating the development of reentrant ventricular arrhythmias during strenuous exercise.

It should be noted that in addition to the identification of p.Gly600Arg in a clinically definite BrS case and now a SUDS victim, the p.Gly600Arg mutation was also recently identified in a single European-American individual by the National Heart Lung and Blood Institute exome-sequencing project (ESP). Thus, p.Gly600Arg appears to be extremely rare (only seen in 1 out of 5379 ESP individuals sequenced). Without demographic and clinical information on the additional p.Gly600Arg-positive individual identified in the ESP, it is difficult to assess the full impact of this additional finding.

Interestingly, to date, pathogenic mutations in *KCND3* have only been identified in males. However, given the skewed male-to-female ratio of our BrS, SIDS, and SUDS cohorts, the proportion of males (4/326, 1.2%) compared with females (0/175, 0%, $P = 0.18$) that harbor a pathogenic *KCND3* mutation failed to reach statistical significance. Although this distribution is likely the result of the overrepresentation of males within these cohorts, one could also speculate that significantly higher baseline expression of *KCND3* in the RV epicardium of males [Di Diego et al., 2002] predisposes those with genetically enhanced I_{to}-mediated transmural voltage gradient to be more susceptible to the development of potentially fatal reentrant ventricular arrhythmias. Physiologic changes during sleep or strenuous exercise that alter the balance of inward (I_{Na} and $I_{L,\,Ca}$) and outward (I_{to} and I_{K-ATP}) currents would be more likely to precipitate a fatal arrhythmia in males harboring *KCND3* mutations than females; thus, it is not entirely surprising that both the p.Val392Ile-positive and p.Gly600Arg-positive SUDS victims were male.

Study Limitations

Although we provide compelling molecular and functional evidence to establish an association between SUDS and *KCND3* mutations, there are some inherent limitations in the present study. First, because of the very definition of these autopsy-negative SIDS and SIDS cohorts, generally none of these victims have ever had premortem cardiological investigations. Therefore, there are no 12-lead ECGs, stress tests, and BrS drug challenges to compare the genotype with a manifest arrhythmia phenotype as there are in studies

involving the living. Clearly, the lack of clinical context further complicates our ability to discern rare SCD-predisposing pathogenic mutations from equally rare yet innocuous background genetic variants identified in autopsy-negative SIDS and SUDS cases. Although the pretest probability that a given rare variant in an established channelopathy-susceptibility gene is pathogenic is expected to be lower when identified in a SUD victim compared with its discovery in an individual with a clinically diagnosed channelopathy, given that cardiac channelopathies underlie a significant subset of SUDS cases (i.e., ~30%); the pretest probability of this same rare variant being pathogenic is much higher if identified in a SUD victim than an ostensibly healthy control, especially when accompanied by cellular electrophysiological data demonstrating a clear functional perturbation. Nevertheless, because of the lack of a clear clinical phenotype, we are only able to demonstrate the association of a potentially proarrhythmic genotype with certain cases of autopsy-negative SIDS/SUDS.

Second, the electrophysiological data in this study were generated by heterologously coexpressing the Kv4.3 channel with the KChIP2 β-subunit in HEK293cells and thus does not completely recapitulate the physiological environment found in human cardiomyocytes. Given the cytosolic carboxyl (C)-terminal location of many of the mutations identified in SIDS/SUDS victims and the fact that the I_{to} current is conducted by a large macromolecular complex in the heart, we cannot completely rule out that the rare p.Ser530Pro variant, which we have classified conservatively as innocuous based upon its WT in vitro properties, might confer channel malfunction in the native cardiomyocyte environment.

Conclusion

This study provides the first direct molecular and functional evidence implicating two missense mutations (p.Val392Ile and p.Gly600Arg) in *KCND3* that perturb the I_{to} current as rare novel pathogenic substrates for SUDS. The precise clinical manifestation of Kv4.3 mutations with loss-of-function and mixed electrophysiological phenotypes remains undefined; further scrutiny will certainly enhance our understanding of the role of the I_{to} current in human disease.

Acknowledgments

We would like to gratefully acknowledge the medical examiners, coroners, and forensic pathologists across the United States for their referral of SUDS and SIDS cases.

Contract grant sponsors: Windland Smith Rice Comprehensive Sudden Cardiac Death Program (M.J.A.); the Dr. Scholl Foundation (M.J.A.); Hannah Wernke Memorial Foundation (M.J.A.); and the National Institutes of Health (R01-HD42569 to M.J.A., R01-HL47678 to C.A., and F30-HL106993 to J.R.G.).

References

Alders M, Koopmann TT, Christiaans I, Postema PG, Beekman L, Tanck MW, Zeppenfeld K, Loh P, Koch KT, Demolombe S, Mannens MM, Bezzina CR, Wilde AA. Haplotype-sharing analysis implicates chromosome 7q36 harboring DPP6 in familial idiopathic ventricular fibrillation. Am J Hum Genet. 2009; 84:468–476. [PubMed: 19285295]

Amin AS, de Groot EA, Ruijter JM, Wilde AA, Tan HL. Exercise-induced ECG changes in Brugada syndrome. Circ Arrhythm Electrophysiol. 2009; 2:531–539. [PubMed: 19843921]

Antzelevitch C, Yan GX. J wave syndromes. Heart Rhythm. 2010; 7:549–558. [PubMed: 20153265]

Arnestad M, Vege A, Rognum TO. Evaluation of diagnostic tools applied in the examination of sudden unexpected deaths in infancy and early childhood. Forensic Sci Int. 2002; 125:262–268. [PubMed: 11909674]

Chugh SS, Reinier K, Teodorescu C, Evanado A, Kehr E, Al Samara M, Mariani R, Gunson K, Jui J. Epidemiology of sudden cardiac death: Clinical and research implications. Prog Cardiovasc Dis. 2008; 51:213–228. [PubMed: 19026856]

Cote A, Russo P, Michaud J. Sudden unexpected deaths in infancy: What are the causes? J Pediatr. 1999; 135:437–443. [PubMed: 10518077]

Delpon E, Cordeiro JM, Nunez L, Thomsen PE, Guerchicoff A, Pollevick GD, Wu Y, Kanters JK, Larsen CT, Hofman-Bang J, Burashnikov E, Christiansen M, Antzelevitch C. Functional effects of KCNE3 mutation and its role in the development of Brugada syndrome. Circ Arrhythm Electrophysiol. 2008; 1:209–218. [PubMed: 19122847]

Di Diego JM, Cordeiro JM, Goodrow RJ, Fish JM, Zygmunt AC, Perez GJ, Scornik FS, Antzelevitch C. Ionic and cellular basis for the predominance of the Brugada syndrome phenotype in males. Circulation. 2002; 106:2004–2011. [PubMed: 12370227]

Dumaine R, Towbin JA, Brugada P, Vatta M, Nesterenko DV, Nesterenko VV, Brugada J, Brugada R, Antzelevitch C. Ionic mechanisms responsible for the electro-cardiographic phenotype of the Brugada syndrome are temperature dependent. Circ Res. 1999; 85:803–809. [PubMed: 10532948]

Gima K, Rudy Y. Ionic current basis of electrocardiographic waveforms: A model study. Circ Res. 2002; 90:889–896. [PubMed: 11988490]

Giudicessi JR, Ye D, Tester DJ, Crotti L, Mugione A, Nesterenko VV, Albertson RM, Antzelevitch C, Schwartz PJ, Ackerman MJ. Transient outward current (I(to)) gain-of-function mutations in the KCND3-encoded Kv4.3 potassium channel and Brugada syndrome. Heart Rhythm. 2011; 8:1024–1032. [PubMed: 21349352]

Klaver EC, Versluijs GM, Wilders R. Cardiac ion channel mutations in the sudden infant death syndrome. Int J Cardiol. 2011; 152:162–170. [PubMed: 21215473]

Liberthson RR. Sudden death from cardiac causes in children and young adults. N Engl J Med. 1996; 334:1039–1044. [PubMed: 8598843]

Makimoto H, Nakagawa E, Takaki H, Yamada Y, Okamura H, Noda T, Satomi K, Suyama K, Aihara N, Kurita T, Kamakura S, Shimizu W. Augmented ST-segment elevation during recovery from exercise predicts cardiac events in patients with Brugada syndrome. J Am Coll Cardiol. 2010; 56:1576–1584. [PubMed: 21029874]

Soh H, Goldstein SA. I SA channel complexes include four subunits each of DPP6 and Kv4.2. J Biol Chem. 2008; 283:15072–15077. [PubMed: 18364354]

Tan HL, Hofman N, van Langen IM, van der Wal AC, Wilde AA. Sudden unexplained death: Heritability and diagnostic yield of cardiological and genetic examination in surviving relatives. Circulation. 2005; 112:207–213. [PubMed: 15998675]

Tester DJ, Ackerman MJ. Sudden infant death syndrome: How significant are the cardiac channelopathies? Cardiovasc Res. 2005; 67:388–396. [PubMed: 15913580]

Tester DJ, Ackerman MJ. Postmortem long QT syndrome genetic testing for sudden unexplained death in the young. J Am Coll Cardiol. 2007; 49:240–246. [PubMed: 17222736]

Tester DJ, Spoon DB, Valdivia HH, Makielski JC, Ackerman MJ. Targeted mutational analysis of the RyR2-encoded cardiac ryanodine receptor in sudden unexplained death: A molecular autopsy of 49 medical examiner/coroner's cases. Mayo Clin Proc. 2004; 79:1380–1384. [PubMed: 15544015]

van der Werf C, van Langen IM, Wilde AA. Sudden death in the young: What do we know about it and how to prevent? Circ Arrhythm Electrophysiol. 2010; 3:96–104. [PubMed: 20160177]

Zheng ZJ, Croft JB, Giles WH, Mensah GA. Sudden cardiac death in the United States, 1989 to 1998. Circulation. 2001; 104:2158–2163. [PubMed: 11684624]

Zingman LV, Alekseev AE, Hodgson-Zingman DM, Terzic A. ATP-sensitive potassium channels: Metabolic sensing and cardioprotection. J Appl Physiol. 2007; 103:1888–1893. [PubMed: 17641217]

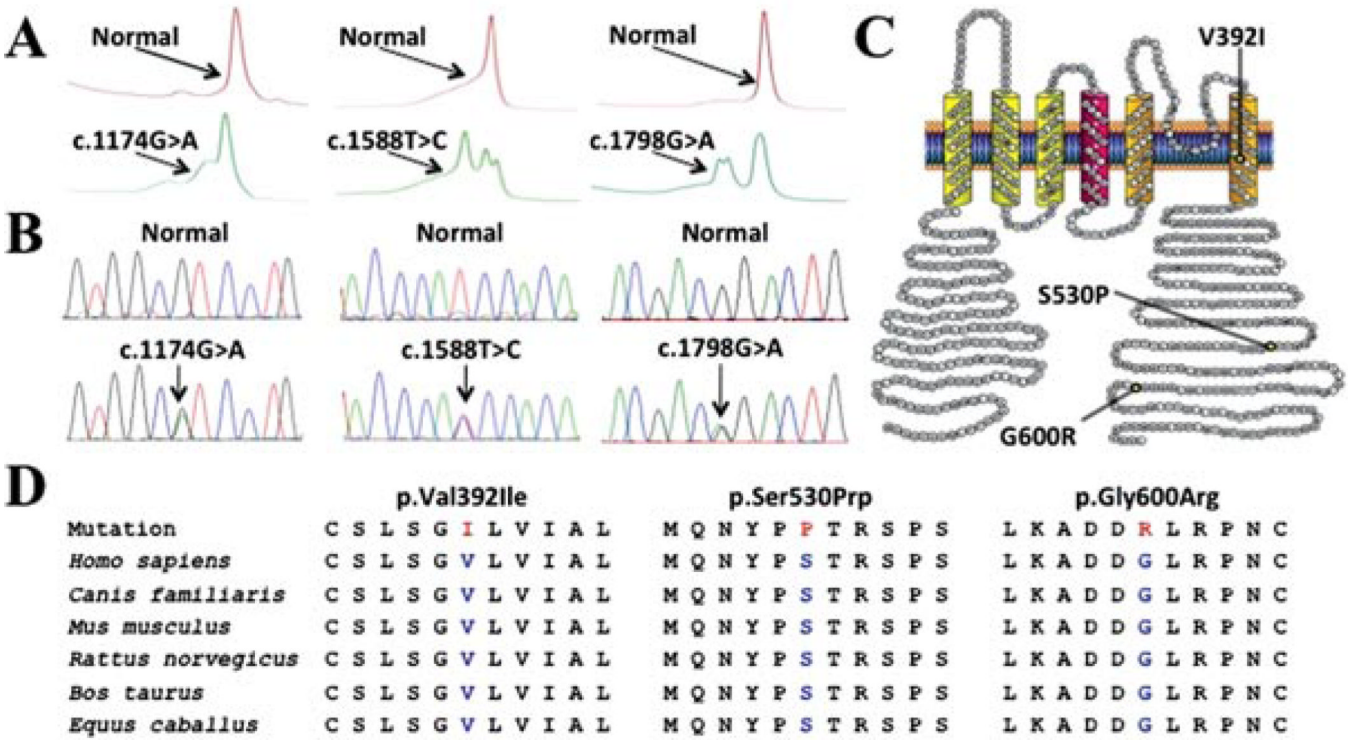

Figure 1.

Identification of SUDS- and SIDS-associated mutations in *KCND3*. Depicted are A: Denaturing high-performance liquid chromatography profiles (normal, red trace; and abnormal, green trace) and B: DNA sequencing chromatographs for c.1174G>A, c. 1588T>C, and c.1798G>A nucleotide substitutions. C: Amino acid sequence conservation across species for p.Val392Ile, p.Ser530Prp, and p.Gly600Arg. D: Predicted protein topology schematic of Kv4.3, indicating the location of the p.Val392Ile, p.Ser530Pro, and p.Gly600Arg missense mutations.

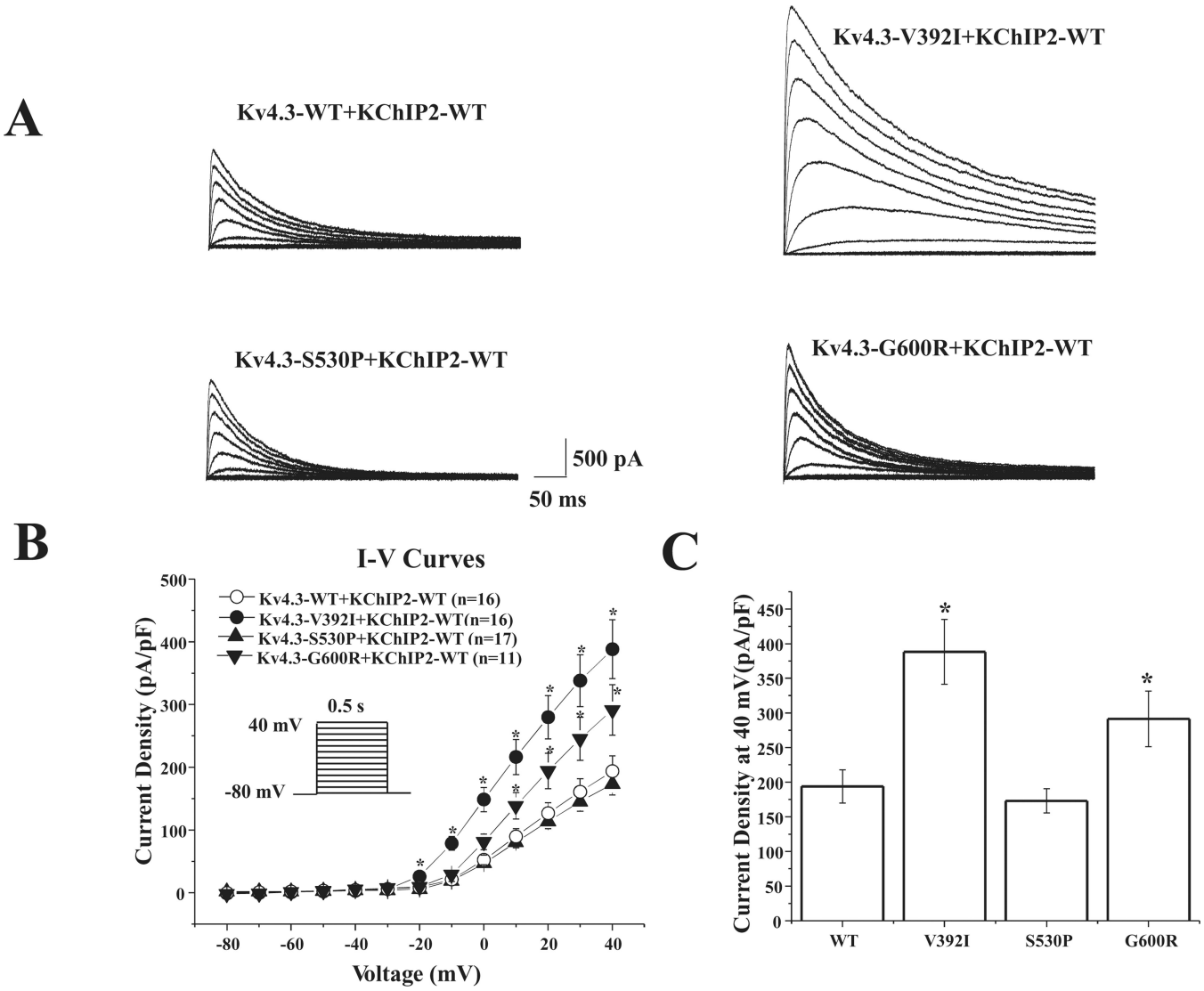

Figure 2.

KCND3 missense mutations increase I_{to} current in heterologous cells. A: Representative whole-cell wild-type (WT) plus KChIP2, p.Val392Ile plus KChIP2, p.Ser530Pro plus KChIP2, and p.Gly600Arg Kv4.3 plus KChIP2 traces recorded in HEK293 cells elicited by step depolarization of 500 ms duration to +40 mV from a holding potential of −80 mV in 10 mV increments. B: The current voltage relationship for WT (n = 16), p.Val392Ile (n = 16), p.Ser530Pro (n = 17), and p.Gly600Arg (n = 11) Kv4.3 channels coexpressed with KChIP2. All values represent mean ± SEM. *P < 0.05 versus WT Kv4.3 plus KChIP2. C: Bar graph showing peak current density at 40 mV for WT (n = 16), p.Val392Ile (n = 16), p.Ser530Pro (n = 17), and p.Gly600Arg (n = 11) Kv4.3 channels coexpressed with KChIP2. *P < 0.05 versus WT Kv4.3 plus KChIP2.

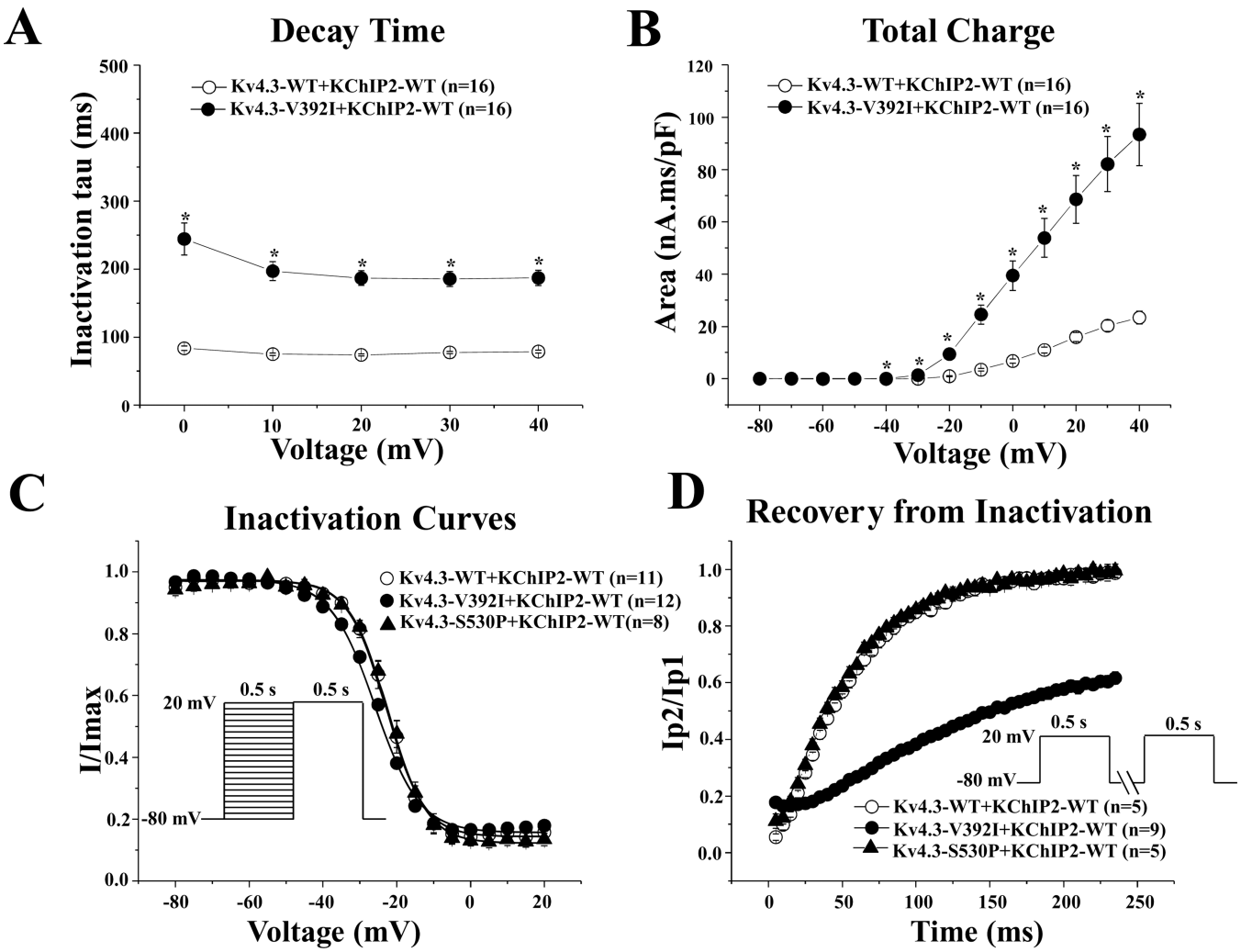

Figure 3.

Kinetic alteration for p.Val392Ile plus KChIP2. A: Inactivation time constants (τ) for wild-type (WT), or p.Val392Ile plus KChIP2 Kv4.3 currents as a function of voltage. Inactivation time constants for each voltage step were determined by fitting a monoexponential function to current decay. All values represent mean ± SEM. *$P < 0.05$ versus WT Kv4.3 plus KChIP2. B: Total charge of WT, or p.Val392Ile with KChIP2 as a function of voltage obtained by measuring the area under curve during the first 50 ms of each voltage step. *$P < 0.05$ versus WT Kv4.3 plus KChIP2. C: Steady-state inactivation curves of WT, p.Val392Ile, or p.Ser530Prp Kv4.3 with KChIP2 determined from a holding potential of −80 mV to prepulse of +20 mV in 5 mV increments with 0.5 s duration followed by a test pulse of +20 mV with 0.5 s duration and fitted with a Boltzmann function. D: Recovery from inactivation of WT, p.Val392Ile, or p.Ser530Pro Kv4.3 with KChIP2 determined from a holding potential of −80 mV to prepulse of +20 mV with 0.5 s duration, with increased recovery interval, followed by a test pulse of +20 mV with 0.5 s duration and fitted with a one-exponential function. All values shown represent mean ± SEM.

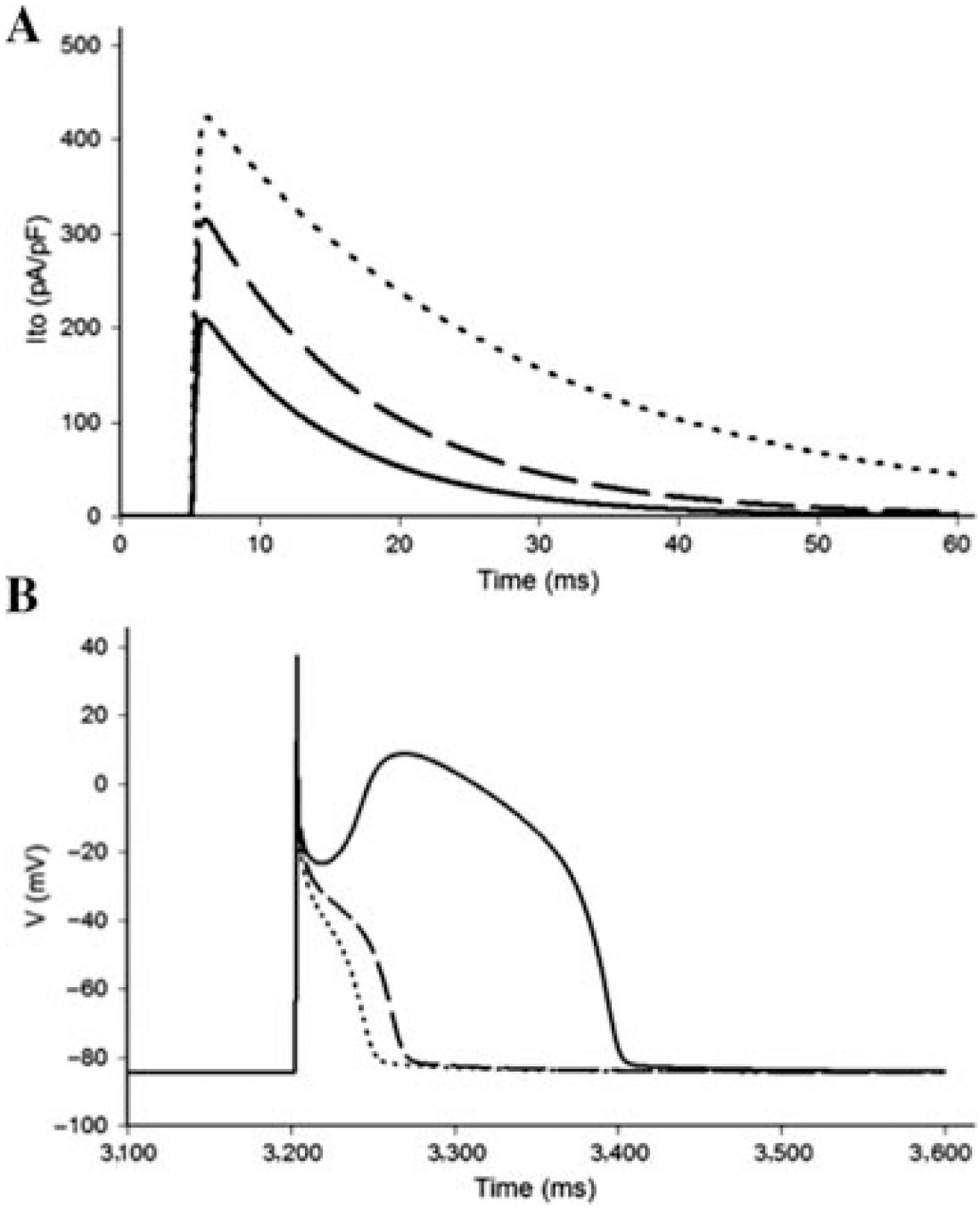

Figure 4.

Effects of p.Val392Ile and p.Gly600Arg on the right ventricular epicardial action potential. A: Simulated I_{to} current traces during step depolarization for 100 ms to 0 mV from a holding potential of −90 mV. Only first 60 ms are shown. Solid line, wild-type (WT); dashed line, p.Gly600Arg; dotted line, p.Val392Ile. B: Right ventricular epicardial action potentials simulated using WT, p.Gly600Arg, and p.Val392Ile mutant I_{to} incorporated into a modified Luo–Rudy II AP model. BCL = 800 ms (75 bpm). Solid line, WT; dashed line, p.Gly600Arg; dotted line, p.Val392Ile. Only the fifth AP in the equilibration chain is displayed here, the AP shape does not change in subsequent cycles.

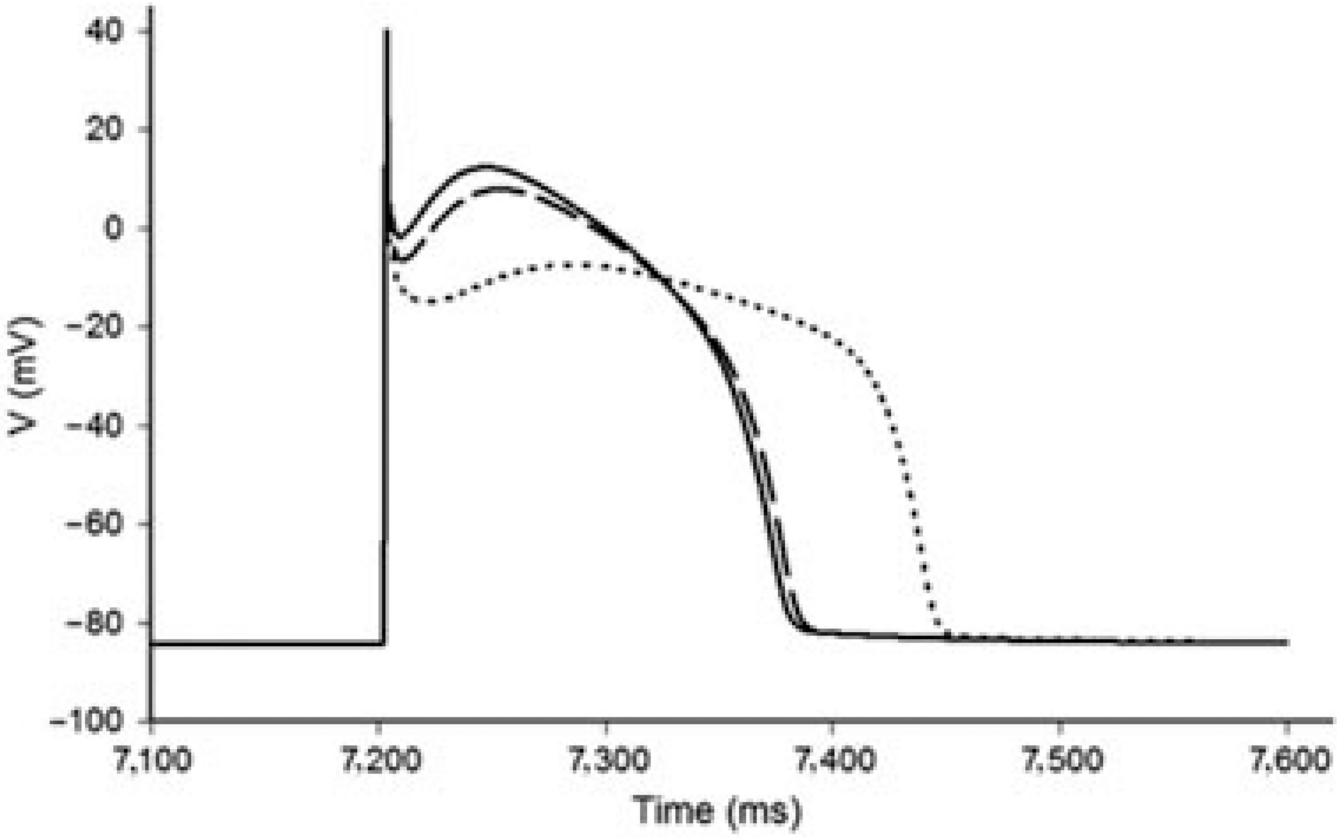

Figure 5.
Simulated effect of p.Val392Ile Kv4.3 on the left ventricular epicardial action potential. Left ventricular epicardial action potentials were simulated using wild-type (WT), p.Gly600Arg, and p.Val392Ile mutant I_{to} incorporated into a modified Luo–Rudy II AP model. BCL = 800 ms (75 bpm). Solid line, WT; dashed line, p.Gly600Arg; dotted line, p.Val392Ile. Only the 10th AP in the equilibration chain is displayed here, the AP shape does not change in subsequent cycles (BCL = 800 ms).

Table 1

Demographics of SUDS Cohort

	SUDS cases
Number of cases	123
Gender	
Male	75
Female	48
Age at death	
Mean (years)	17.5 ± 12.3
Range (years)	1–69
Reported ethnicity	
Caucasian	108
African American	10
Hispanic	2
Asian	3

[a]Although no upper age limit was specified to accept a sample for postmortem genetic testing, 112 of the 123 cases were between 1 and 40 years of age. Seven decedents were in their 40s, three were in their 50s, and a single SUD victim was in his 60s.

Table 2

Demographics of SIDS Cohort

	SUDS cases
Number of cases	292
Gender	
Male	178
Female	114
Age at death	
Mean (months)	2.9 ± 1.9
Range (months)	0.1–12
Reported ethnicity	
Caucasian	204
African American	76
Hispanic	10
Asian	2

Table 3

KCND3 Mutations Identified in SIDS and SUDS Cases

Case description	Nucleotide change	Amino acid change	Localization	Electrophysiological phenotype
20-Year-old Caucasian male SUDS victim	c.1174G>A	p.Val392Ile	Transmembrane	Mixed
2-Month-old African American male SIDS victim	c.1588T>C	p.Ser530Pro	C-terminal	Wild-type
23-Year-old Caucasian male SUDS victim	c.1798G>A	p.Gly600Arg	C-terminal	Gain-of-function